JSEE Vol. 22, No. 4, 2020 DOI: 10.48303/jsee.2022.249405

Research Paper

Seismic Responses of Innovative Vertically Isolated Liquid Storage Tanks under Near-Fault and Far-Fault Ground Motions

Morteza Moeini[1] and Mohammad Ali Goudarzi[2*]

1. Assistant Professor, University of Zanjan, Zanjan, Iran
2. Associate Professor, Structural Engineering Research Center, International Institute of Earthquake Engineering and Seismology (IIEES), Tehran, Iran,
*Corresponding Author; email: m.a.goodarzi@iiees.ac.ir

Received: 09/09/2020
Revised: 19/10/2021
Accepted: 24/01/2022

ABSTRACT

The seismic response of aboveground liquid storage tanks isolated by the proposed vertical isolation system (VIS) is investigated under near-fault and far-fault ground motions. For this purpose, a set of 14 ground motions including seven far-fault and seven pulse-like near-fault motions have been considered. Effectiveness of VIS is evaluated theoretically and numerically in selected tanks with different geometries including Short-Broad, Tall-Broad, Short-Slender, and Tall-Slender. In the proposed isolation system, the tank shell is detached from the base and supported on a ring of vertical isolators, and then the forces in the vertical direction caused by the over-turning moment are isolated as an alternative to the common horizontal system used for shear base isolation of storage tanks. The equations of motion for a liquid tank equipped with the proposed system were extracted using the mass-spring simplified model of contained liquid. A study was performed by employing the non-linear solution of the governing equations and the effectiveness of the proposed system for selected tanks is discussed. To measure the effectiveness of the isolation system, the seismic response of isolated steel tanks is compared with that of the non-isolated (or fixed-base) tanks. The results of this study demonstrate the influence of the tank's geometries, characteristics of the isolation system, and input excitation features. These parameters should be reasonably selected to achieve the maximum mitigation of seismic responses in the tanks equipped with the VIS. Excitation parameters, PGV/PGA ratio of input records, and pulse period in two sets of ground motions are defined to recognize the variety of responses. It is confirmed that the VIS performs well under both near and far-fault motions but near-fault earthquakes amplify the seismic responses more than the far-fault records especially in broad tanks.

Keywords:
Liquid Storage Tank; Base Isolation; Near-fault and far-fault ground motion

1. Introduction

Aboveground storage tanks (ASTs) have an important role in lifelines, industries, petrochemical, and power plants. During past earthquakes, ASTs suffered from different types of failure modes such as shell buckling, roof damages, anchor bolts, and nozzle failure, sliding, and uplifting [1-4]. Then maintaining their stability and improving their overall seismic performances requires special attention. There are two different approaches in enhancing the seismic performances of ASTs included: Conventional and Moderate retrofit methods.

Conventional retrofit methods strengthen the individual elements of a structure while moderate methods improve the overall seismic behavior. Because of the high aspect ratio (H/D) and low radius to thickness (r/t), the cylindrical steel storage tanks are vulnerable to the shell buckling phenomenon. Shell buckling comprises diamond-shaped and

elephant-foot buckling. The critical buckling mode mainly depends on the geometric parameters including tank height (H) and the tank aspect ratio (H/D) [5]. Conventional rehabilitation methods such as adding FRP composite material to the tank shell have been proposed in recent years and its effects on the shell buckling have been investigated by researchers [6-9]. Also, in another retrofitting method, Chen et al. [10] proposed a simple method in which a light ring stiffener is used at a critical location. It has been shown that the location and size of the ring must be chosen with care and that a very light ring is generally sufficient to produce a significant improvement.

Moderate methods such as base isolation systems improve the overall seismic behavior of structures. Generally, isolators can be classified as elastomeric and sliding types. One of the first experimental studies on the base isolation of ASTs was performed by Chalhoube and Kelly [11] in 1988, in which the seismic behavior of two similar tanks was compared with each other. One of the tanks was directly fixed to the shake table and the other was mounted on the base of the base-isolated nine-story steel structure. The results indicated the benefit of rubber bearing isolation system on the reduction of seismic responses while sloshing height increased slightly. Researchers like Shekari et al. [12], Vosoughifar and Naderi [13], Li et al. [14], Yang et al. [15], and Cheng et al. [16], studied the effects of the rubber isolation system on the seismic behavior of the storage tanks. Their results confirm the beneficial effect of rubber bearing on the mitigation of seismic responses. Wang et al. [17] used extensive numerical simulations to assess the effectiveness of seismic base isolation for rigid cylindrical tanks using sliding isolators. The results showed the effectiveness of the sliding isolation system on the reduction of impulsive dynamic pressure while barely affecting the convective dynamic pressure. Park et al. [18] studied the influence of site and seismicity on the efficiency of isolating systems. They concluded that sliding isolation is more effective in rock sites and the region of low to moderate seismicity. Also, the results of the other researchers such as Shirmali and Jangid [19-20], Jadhav and Jangid [21], Wen et al. [22], Zhang et al. [23], and Cheng et al. [24] showed that the application of sliding isolators can improve the seismic behavior of storage tanks. The seismic response of liquid storage steel tanks isolated with Variable Frequency Pendulum Isolator (VFPI) and Friction Pendulum System (FPI) is investigated under six recorded near-fault ground motions by Panchal and Jangid [25]. It has been concluded that the base shear, the sloshing displacement, and the impulsive displacement during near-fault ground motions can be controlled within a desirable range. Safari and Tarinejad [26] evaluated the seismic response of base-isolated steel liquid storage tanks under the near and far-fault excitation by a stochastic approach in the frequency domain. The results showed that the near-fault earthquake excitations amplify the overall response of the system. It was observed that the sloshing responses of the tanks are significantly reduced by sliding bearing.

All of these studies focus on horizontal base isolation in ASTs. Horizontal isolation of the tank base decreases the base shear and the overturning moment, which is the source of vertical seismic stress in a tank shell. Nikoomanesh et al. [27] proposed a new isolation system in which the vertical forces produced by the overturning moments are directly isolated and the buckling stress is mitigated. The effects of their proposed method were studied numerically via finite element methods. In another study, Moeini et al. [28] investigated the effect of their proposed vertically isolation system (VIS) on the practical range of tanks geometries via a theoretical numerically approach. The results showed that the proposed VIS can reduce the overturning moment up to 90%.

In the current study, the performances of the proposed VIS system under the excitation of near and far-field ground motion are investigated. For this purpose, two sets of earthquakes included near and far-fault records are defined to recognize the variety of responses. To compare the effect of the proposed system, the seismic responses of isolated and corresponding fixed-based tanks are compared. The results showed that the VIS performs well in both sets of records and causes a significant reduction in seismic responses.

2. Characteristics of Input Seismic Ground Motions

The release of abrupt energy in the vicinity of faults rupture is associated with the generation of ground motions. Characteristics of ground motions

may differ in case of effective parameters such as magnitude, source mechanism, propagation path of wave, distance and direction from the fault location and site soil condition [29]. Bolt used the term "near-fault" for the first time to specify the structural responses due to strong shakes in the locality of faults [30]. In general, special features of near-fault earthquakes are directivity effect and fling step that both occur parallel to the strike of the fault for strike-slip earthquakes and in the dip direction for dip-slip events. A unidirectional large-amplitude velocity pulse and a discrete step in the displacement time history are the characteristics of the fling step phenomenon. Directivity effects are classified to forward, reverse, and neutral directivity effects (site A, B, and C in Figure (1) respectively) [31]. The rupture often propagates at a velocity close to the velocity of shear wave radiation and then the energy is accumulated in front of the propagating rupture and is expressed in the forward directivity region as a large velocity pulse with a high period [32]. Generally, this sort of motion represents peak velocity and period higher than 50 cm/sec and 1 sec respectively, and it appears in fault normal direction due to the reflexive pattern of shear displacement [33]. Two sets of near and far-fault records are selected to recognize the variation of responses. The records are obtained from the PEER database [34] according to the recommendation of FEMA P695-Appendix A [35]. The properties of these records are represented in Tables (1).

It should be noted that the real earthquake without any scaling factor is used here because the scaling changes the peak ground velocity, which is one of the most important factors in seismic responses especially in near field long period records [36].

The average acceleration response spectrum with a damping ratio of 5% for selected near-fault and far-fault ground motion records are presented in Figure (2). The response spectrum of near-fault ground motions possesses two peaks amplitude in both high and low frequencies.

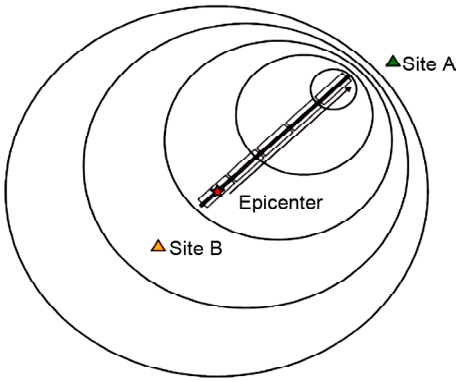

Figure 1. Directivity effect in fault rupture site [31].

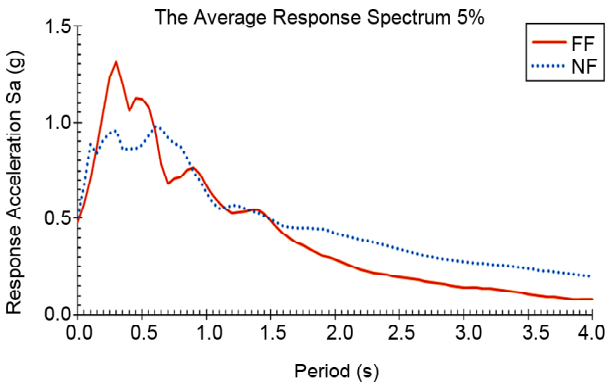

Figure 2. Average acceleration response spectrum.

Table 1. Characteristics of far-fault (FF) and near-fault ground motions.

ID No.	Event	M_w	Fault Type	Station	Closest (Km)	Angle	PGA (g)	PGV (cm/s)	PGD (cm)	PGV/PGA	PGV/PGD
Far-Field Records											
1 (FF1)	1994 Northridge	6.7	Thrust	Mulhol	17.2	279	0.52	62.77	11.07	120.71	5.67
2 (FF2)	1999 Duzce, Turkey	7.1	Strike-Slip	Bolu	12	0	0.73	56.44	23.08	77.32	2.45
3 (FF3)	1979 Imperial Valley	6.5	Strike-Slip	El Centro Array #11	12.5	140	0.36	34.44	16.08	95.67	2.14
4 (FF4)	1999 Kocaeli, Turkey	7.5	Strike-Slip	Duzce	15.4	270	0.36	46.39	17.68	128.86	2.62
5 (FF5)	1992 Cape Mendocino	7.0	Thrust	Rio Dell Overpass	14.3	270	0.38	43.80	21.65	115.26	2.02
6 (FF6)	1995 Kobe, Japan	6.9	Strike-Slip	Nishi-Akashi	7.1	90	0.50	36.63	11.25	73.26	3.26
7 (FF7)	1990 Manjil, Iran	7.4	Strike-Slip	Abbar	12.6	90	0.49	52.09	20.77	106.31	2.51
Near-Field Records											
8 (NF1)	1994 Northridge	6.7	Thrust	Sylmar - Olive View	5.3	32	0.60	78.10	16.82	130.17	4.64
9 (NF2)	1999 Duzce, Turkey	7.1	Strike-Slip	Duzce	6.6	262	0.54	83.51	51.62	154.65	1.62
10 (NF3)	1979 Imperial Valley	6.5	Strike-Slip	El Centro Array #6	1.4	323	0.44	109.82	65.83	249.59	1.67
11 (NF4)	1999 Kocaeli, Turkey	7.5	Strike-Slip	Izmit	7.2	270	0.15	22.60	9.79	150.67	2.31
12 (NF5)	1992 Cape Mendocino	7.0	Thrust	Petrolia	8.2	350	0.66	89.68	28.99	135.88	3.09
13 (NF6)	1992 Landers	7.3	Strike-Slip	Lucerne	2.2	260	0.73	146.50	262.73	200.68	0.56
14 (NF7)	1987 Superstition Hills	6.5	Strike-Slip	Parachute Test Site	1.0	37	0.45	111.99	52.75	248.87	2.12

3. Proposed Vertical Isolation System

On the contrary to the typical horizontal isolation system, the proposed system performs in the vertical direction. Common isolation systems horizontally separate a structure from its base while the proposed isolation system has vertically detached the shell from the base and support it on vertical isolators (Figure 3). Disconnecting the tank shell from the base plate isolates the rocking motion of an AST, and it can eliminate the need for a solid base for isolation of the entire base plate required in the common horizontal isolation system. Then the number of isolation elements required decreases significantly with respect to the common horizontal isolation and these differences lead to the significant reduction in the cost of implementation of base isolation in practice. Since the base plate is not attached to the tank wall, the hydrodynamic pressure at the base plate will not be transferred to the foundation. Therefore, plastic rotations, which are a common problem in conventional tanks, will not occur at the tank wall-base plate connections and base plate rupture will be avoided [27].

At the intersection of shell and base plate in VIS leakage can occur. A flexible membrane (such as synthetic membranes) between the shell and the base plate is proposed to solve this problem as depicted schematically in Figure (4). A filling replaceable material is placed between the soil and tank shell to prevent horizontal movement but it permits the rocking motion in the tank shell wall. This filling material can be chosen from Styrofoam material. A space (void) underneath the filling material is provided, which allows the shell wall to move freely during ground motions showed schematically with rolling supports in Figure (4b).

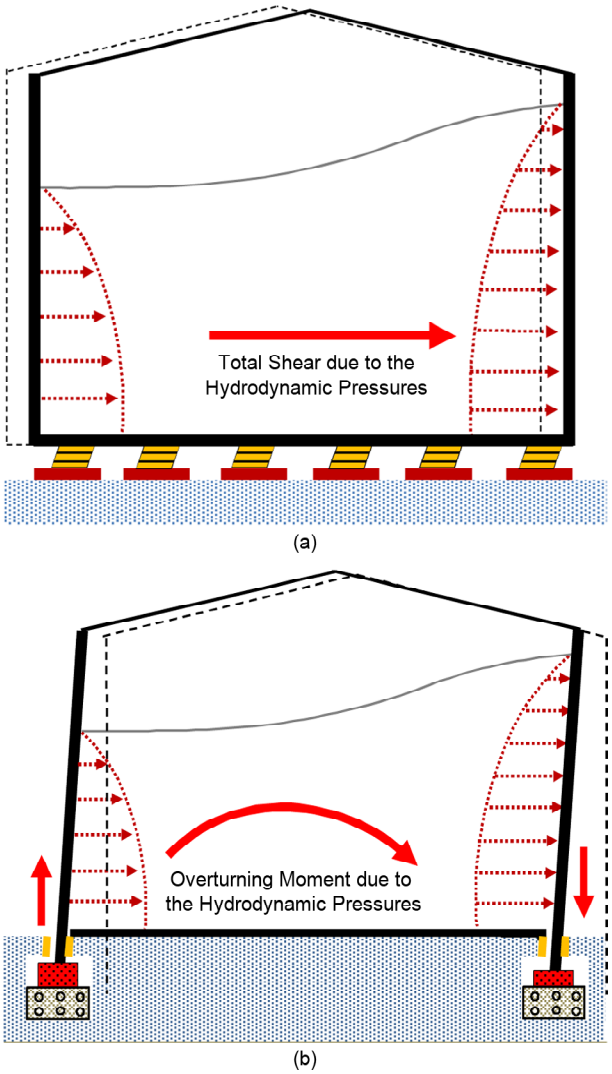

Figure 3. Schematic of typical horizontal isolation and proposed vertical isolation [27].

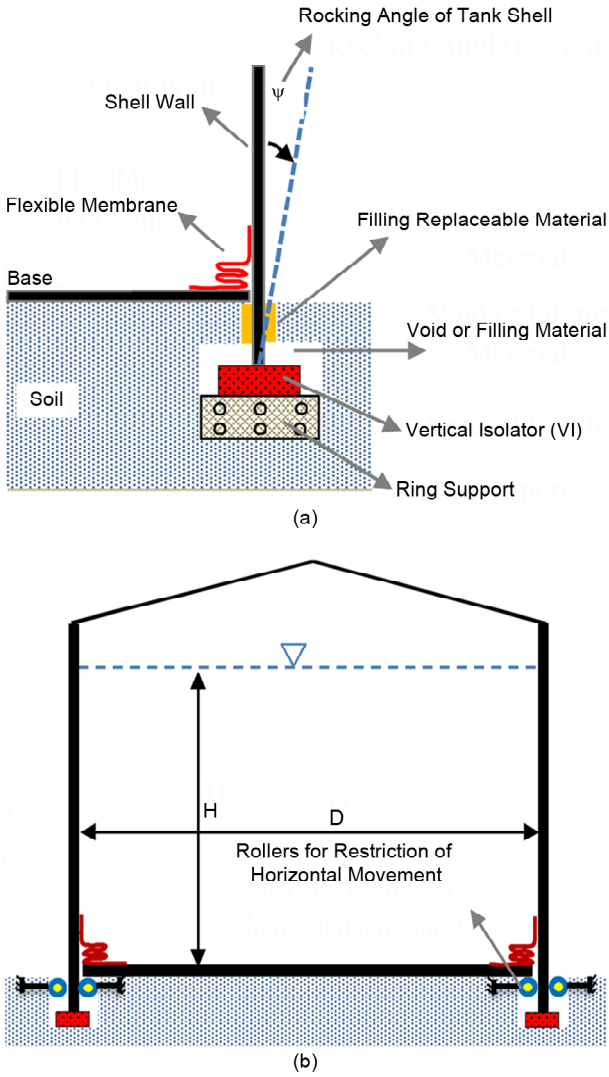

Figure 4. Details of VIS at the intersection of the shell and bas plate [27].

4. Extraction Equations of Motion

A simplified Equivalent mass-spring model that captures the essential dynamic characteristics of the isolated system is shown in Figure (5). The system examined is an ASTs of radius R, which is filled to a height H, with a liquid of mass density ρ_l. The tank is presumed to rest on a series of rigid beams uniformly spaced along the bottom plate boundary. In this model, m_i and m_c are the impulsive and convective (sloshing) masses. The natural frequencies of the fixed-base impulsive and convective responses are denoted by ω_i and ω_c and the respective damping ratios are denoted by ξ_i and ξ_c; h_i and h_c are the heights of the resultant of the hydrodynamic wall pressures due to impulsive and convective actions. The values of m_i, m_c, h_i, h_c, ω_i, and ω_c can be obtained from the results of Veletsos and Tang [37]. For steel tanks, the impulsive damping ratio is assumed to be $\xi_i = 0.02$ and the convective damping ratio is assumed $\xi_c = 0.05$. It approved that the simplified mechanical models can be used with confidence for evaluating the seismic design parameters of various isolated tanks and the difference between the base shear and overturning moment results in the FE model and the simplified model of an isolated tank limited to 10% [38].

$$\omega_i = \frac{P}{H}\sqrt{E/\rho_l} \tag{1}$$

$$\omega_c = \frac{2\pi}{T_c} = \sqrt{\lambda_i \tanh(\lambda_i H/R)(g/R)} \tag{2}$$

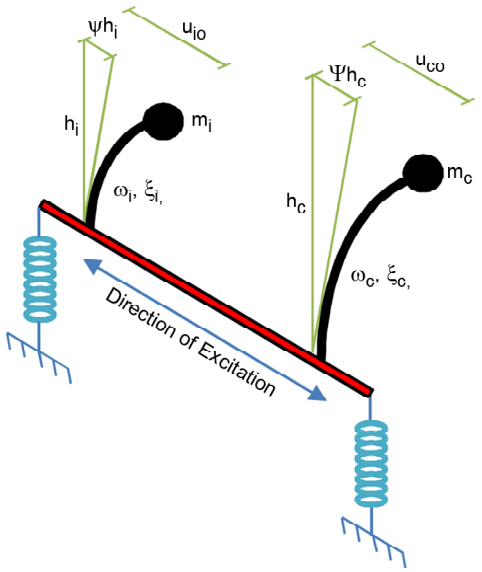

Figure 5. Simplified model of VIS.

$$k_{imp} = m_i\omega_i^{\,2}, \qquad k_{con} = m_c\omega_c^{\,2} \tag{3}$$

$$C_{imp} = 2m_i\omega_i\xi_i, \qquad C_{con} = 2m_c\omega_c\xi_c \tag{4}$$

where E is the modulus of elasticity, P is a dimensionless parameter expressed by $P=0.037085+0.084302(H/R) - 0.05088(H/R)^2 + 0.012523(H/R)^3 - 0.0012(H/R)^4$; λ_i is the ith zero of the first derivative of the Bessel function of the first kind of the first order. The first three values of λ_i are: $\lambda_1 = 1.841$, $\lambda_2 = 5.331$ and $\lambda_3 = 8.536$; k_{imp} and k_{con} are fixed-base impulsive and convective stiffness, respectively, C_{imp} and C_{con} are fixed-base impulsive and convective damping factors, respectively. The dynamic equilibrium of forces on the masses m_i and m_c can be written as:

$$m_i\ddot{u}_{io} + C_{imp}\left(\dot{u}_{io} - h_i\dot{\psi}\right) + k_{imp}\left(u_{io} - h_i\psi\right) = -m_i\ddot{x}_g(t) \tag{5}$$

$$m_i\ddot{u}_{co} + C_{con}\left(\dot{u}_{co} - h_i\dot{\psi}\right) + k_{con}\left(u_{co} - h_c\psi\right) = -m_c\ddot{x}_g(t) \tag{6}$$

Another required equation can be derived by considering the equilibrium of base moments as:

$$2R\sum_{i=1}^{\frac{n}{2}-1} f_i(t)\sin\left(\frac{2\pi i}{n}\right) - \left[C_{imp}\left(\dot{u}_{io} - h_i\dot{\psi}\right) + k_{imp}\left(u_{io} - h_i\psi\right)\right]h_i - \left[C_{con}\left(\dot{u}_{co} - h_c\dot{\psi}\right) + k_{con}\left(u_{co} - h_c\psi\right)\right]h_c = 0 \tag{7}$$

where u_{io} and u_{co} are overall impulsive and convective horizontal displacements of masses relative to moving base respectively, ψ is the rotation of tank base and an over dot denotes differentiation with respect to time, $\ddot{x}_g(t)$ is ground acceleration, R is the tank radius, n is the number of isolators provided under the tank shell and $f_i(t)$ is the reaction force of each isolator according to the presumed isolators force-deflection behavior respect to the time. Equations (5) to (7) are solved incrementally through a numerical linear acceleration method.

5. Characteristics of Isolation System

Although different hypotheses on the constitutive law for the isolation devices have been developed, a bilinear force-deformation behavior is generally recommended for the base isolating model in most

cases to simplify the design procedure [39]. The system can be characterized by several parameters including the initial elastic stiffness K_e, post-elastic stiffness K_p, the strain hardening ratio α, characteristic strength Q_y, the yield strength F_y, yield displacement Δ_y, and maximum bearing displacement Δ_{max}, as presented in Figure (6).

Rosenblueth and Herrera [40] firstly proposed the secant stiffness at maximum deformation as the basis for selecting the period ratio. Considering the idealized bilinear hysteresis model, the equivalent stiffness can be determined based upon the concept of secant stiffness:

$$K_{eq} = F_d / \Delta_{max} \tag{8}$$

where

$$F_d = K_e \Delta_y + K_p \left(\Delta_{max} - \Delta_y\right) \tag{9}$$

Therefore,

$$K_{eq} = \left[K_e \Delta_y + K_p \left(\Delta_{max} - \Delta_y\right)\right] / \Delta_{max} = K_e \left[\frac{\Delta_y}{\Delta_{max}} - \frac{K_p}{K_e}\left(1 - \frac{\Delta_y}{\Delta_{max}}\right)\right] \tag{10}$$

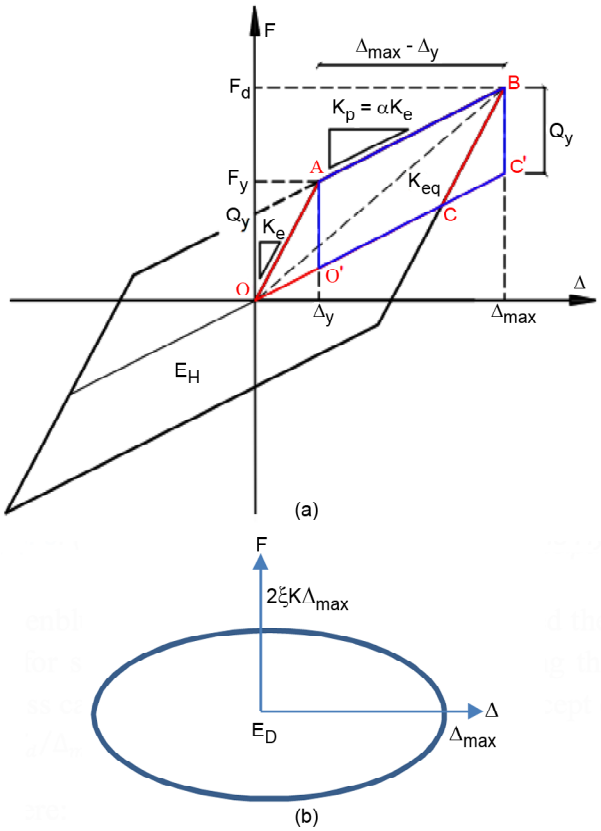

Figure 6. (a) The concept of secant stiffness and the Hysteresis energy dissipated by one cycle in bilinear hysteretic model (b) Damping energy dissipated by one cycle f harmonic response [39]

If $\mu = \frac{\Delta_{max}}{\Delta_y}$ and $\alpha = \frac{K_p}{K_e}$, substitute them in above above equation leads to:

$$K_{eq} = K_e \left[\frac{1}{\mu} - \alpha\left(1 - \frac{1}{\mu}\right)\right] = K_e \frac{1 + \alpha(\mu - 1)}{\mu} \tag{11}$$

Once the equivalent stiffness is determined, the equivalent period and initial period can be computed using the following equations, respectively:

$$T_{eq} = 2\pi\sqrt{M / K_{eq}}, \qquad T_i = 2\pi\sqrt{M / K_e} \tag{12}$$

where M is the total mass of the isolation system, including the mass of the superstructure and the mass of the isolation system [21]. Hysteretic damping can be determined by equating the energy dissipated by one cycle of the bilinear model with the energy dissipated by one cycle of harmonic response. The hysteresis energy dissipated by one cycle (Figure 6a) can be expressed as:

$$E_H = 4S_{oABC} = 4S_{O'ABC'} = 4Q_y\left(\Delta_{max} - \Delta_y\right) = 4\Delta_y\left(K_e - K_p\right)\left(\Delta_{max} - \Delta_y\right) \tag{13}$$

For linear elastic systems with a damping ratio ξ and a secant stiffness K, the damping energy dissipated by one cycle of harmonic response is defined by the area of the ellipse shown in Figure (6b).

$$E_D = \pi\Delta_{max}\left(2\xi K \Delta_{max}\right) = 2\pi\xi K \Delta_{max}^2 \tag{14}$$

Substituting K_{eg} by K in Equation (14) and employing the equal energy dissipation principle (i.e., $EH = ED$), the hysteretic damping ratio of the equivalent linear systems can be derived:

$$\xi_{hyst} = \frac{E_{hyst}}{2\pi\xi K_{eq}\Delta_{max}^2} = \frac{4\Delta_y\left(K_e - K_p\right)\left(\Delta_{max} - \Delta_y\right)}{2\pi\xi K_{eq}\Delta_{max}^2} = \frac{4\left(1 - K_p / K_e\right)}{2\pi\left(\Delta_{max} / \Delta_y\right)^2}\frac{K_e}{K_{eq}} = \frac{2(1-\alpha)(\mu - 1)}{\pi\mu\left[1 + \alpha(\mu - 1)\right]} \tag{15}$$

If the inherent viscous damping ratio of bilinear systems ξ_0 is considered, the equivalent viscous damping ratio can be finally expressed as:

$$\xi_b = \xi_0 + \xi_{hyst} = \xi_0 + \frac{2(1-\alpha)(\mu - 1)}{\pi\mu\left[1 + \alpha(\mu - 1)\right]} \tag{16}$$

The assumed seismic parameters for the isolators in the current study are $T_{iso} = 2s$ and $\xi_b = 0.10$ which are recommended in the literature [41].

6. Results and Discussion

In this study, in order to evaluate the efficiency of the proposed VIS, four different tanks with different geometry including Short-Broad (SB), Short-Slender (SS), Tall-Broad (TB) and Tall-Slender (TS) are considered. The aforementioned tanks are analyzed under the near and far-fault excitation according to Table (1). The characteristics of considered tanks and their associated seismic specifications are presented in Table (2). The modulus of elasticity, Poisson's ratio and mass density of tanks are 200 GPa, 0.3 and 7850 kg/m^3, respectively. Considered tanks are equipped with the VIS isolators and their seismic response are compared with their corresponding fixed-base tanks. Because of the direct impact of VIS isolators on the overturning moment, the effect of the proposed isolation system is evaluated through this seismic response.

In the proposed isolation system, the tank shell is detached from the base and supported on a ring under the shell wall, so that dampen the rocking motion of the tank shell caused by dynamic loads. On the other hand, the forces in the vertical direction caused by the overturning moment are isolated as an alternative to the common horizontal system used for shear base isolation. The numerical results show that the overturning moment of the tanks equipped with the proposed isolation system decreased significantly with respect to the corresponding fully anchored tanks. The maximum values of the resultant overturning moment in considered tanks under the input excitations are presented in Table (3). The values in this table are obtained from the peaks in the time history responses of each tank.

The amount of reduction in overturning moment responses of isolated tanks in comparison with fix-based ones shows the efficiency of the isolation method. On the other hand, the ratio of the overturning moment in the VIS tank to corresponding rigid tanks (M_{iso}/M_{rigid}) indicates the higher efficiency of the proposed system in each specified

Table 2. Seismic specifications for selected tanks.

Tanks Properties	H (m)	D (m)	H/D	m_i (ton)	m_c (ton)	h_i (m)	h_c (m)	T_i (s)	T_c (s)	k_{imp} (kN/m)	k_{con} (kN/m)	C_{imp} (kN.s/m)	C_{con} (kN.s/m)
Short-Broad (SB)	7.2	24	0.3	1121	1999	2.70	3.92	0.17	5.69	1602578	2436	1695	22
Short-Slender (SS)	7.2	4.8	1.5	111	19.98	3.15	5.90	0.08	2.28	706918	151	354	0.55
Tall-Broad (TB)	16.8	56	0.3	14245	25406	6.30	9.16	0.32	8.69	5559967	13264	11257	183
Tall-Slender (TS)	16.8	11.2	1.5	1414	253	7.35	13.77	0.25	3.48	882926	826	1413	4.58

Table 3. Maximum overturning moment in considered tanks under input exitations.

	ID NO.	Short-Broad (SB)			Tall-Broad (TB)			Short-Slender (SS)			Tall-Slender (TS)		
		M_{iso}	M_{fixed}	Ratio	M_{iso}	M_{fixed}	Ratio	M_{iso}	M_{fixed}	Ratio	M_{iso}	M_{fixed}	Ratio
FF1	1	23.20	37.87	0.61	678.68	1317.24	0.52	0.31	3.33	0.09	8.58	124.01	0.07
FF2	2	17.31	34.56	0.50	538.04	2777.62	0.19	0.24	3.56	0.07	9.11	247.55	0.04
FF3	3	10.02	50.04	0.20	330.66	1088.74	0.30	0.24	2.24	0.11	6.76	218.39	0.03
FF4	4	14.64	20.05	0.73	440.37	894.42	0.49	0.29	1.87	0.16	8.93	125.58	0.07
FF5	5	11.73	33.62	0.35	367.41	1182.37	0.31	0.26	2.10	0.12	6.60	108.63	0.06
FF6	6	14.66	28.72	0.51	480.45	1070.48	0.45	0.22	2.34	0.09	6.28	148.35	0.04
FF7	7	15.49	49.62	0.31	429.93	1501.74	0.29	0.24	5.95	0.04	8.29	172.46	0.05
NF1	8	15.25	29.35	0.52	645.52	1439.48	0.45	0.30	3.00	0.10	10.59	90.80	0.12
NF2	9	20.07	29.94	0.67	514.98	1222.25	0.42	0.74	1.82	0.41	23.08	149.76	0.15
NF3	10	15.26	27.11	0.56	376.06	971.48	0.39	0.58	3.13	0.19	21.54	182.02	0.12
NF4	11	9.42	13.35	0.71	249.98	442.40	0.57	0.18	1.60	0.11	6.32	69.50	0.09
NF5	12	32.23	37.60	0.86	961.08	1240.04	0.78	0.41	3.68	0.11	13.28	93.16	0.14
NF6	13	23.45	48.30	0.49	430.74	1123.41	0.38	0.65	10.62	0.06	24.05	216.65	0.11
NF7	14	15.96	25.88	0.62	450.75	904.30	0.50	0.46	1.89	0.24	19.79	107.43	0.18

tank. By examination of the results of Table (3), it can be concluded that the VIS performs better in the slender tanks rather than the broad ones. As an example, the time history responses of the overturning moment in selected tanks under the near-fault and far-fault records of the Imperial Valley earthquake (FF3 & NF3) as an input excitation are presented in Figure (7) for the base-isolated and corresponding fixed-base tanks. It can be concluded that the near-fault motions have higher overturning moment in comparison to the far-fault records in most cases. As will be shown, vertical isolation increases the effective damping of ASTs by more than 20%, which is much greater than the fixed-base impulsive damping value of 2% (Figure 8). Also, VIS increases the effective impulsive period, it can be seen from

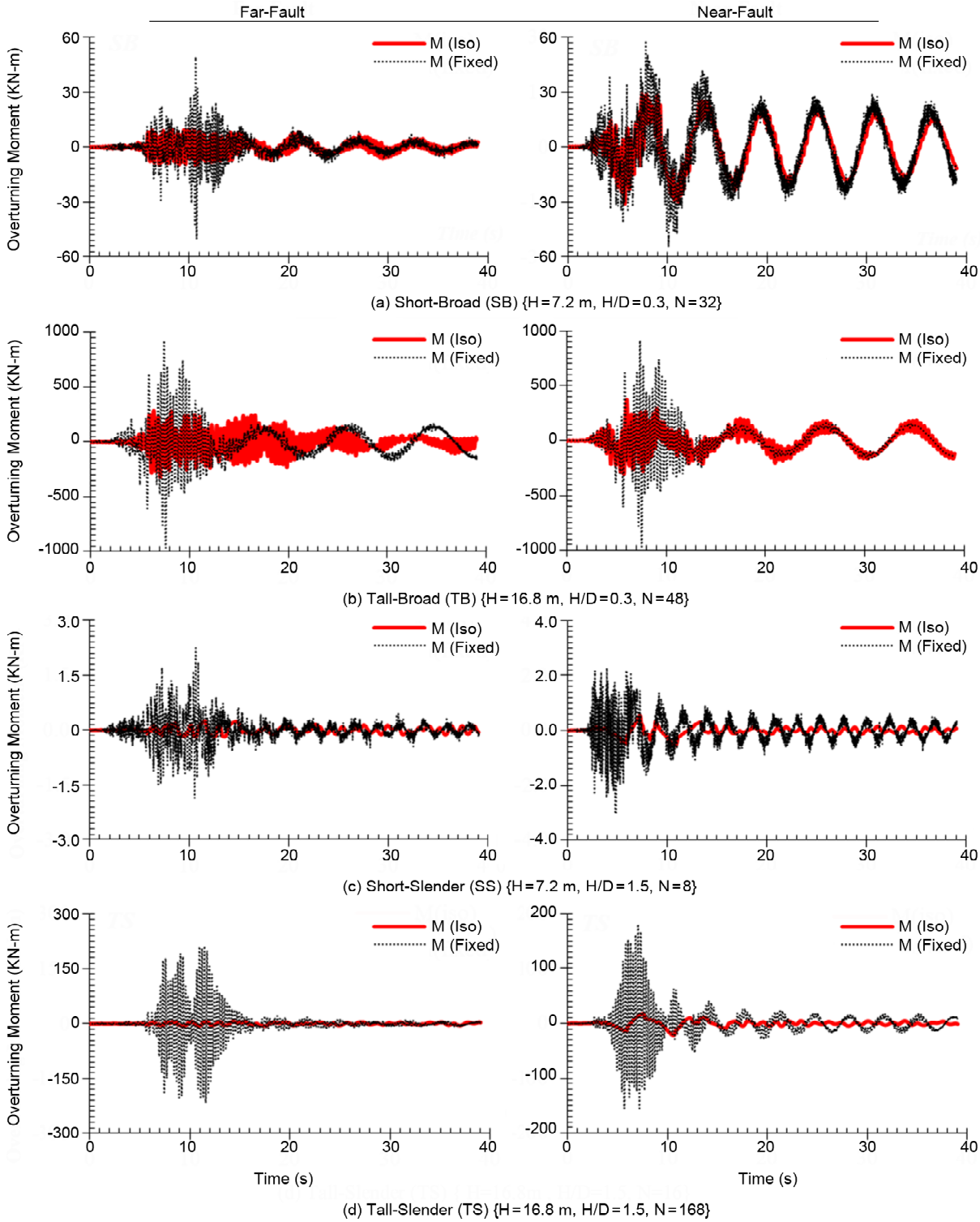

Figure 7. Time history responses of overturning moment in seleted tanks under FF3 and NF3 input records.

the response spectra plotted in Figure (2) that an increase in the period often decreases spectral acceleration SA (g). The resultant of these changes lead to a significant reduction in isolated tanks. Besides, it can be said that the rigid broad tanks have the higher impulsive period rather than rigid slender tanks. Then, increasing the period as a result of isolation leads to a smaller reduction in spectral acceleration in broad tanks. Finally, these differences lead to the lower performances of broad tanks rather than slender tanks.

The equivalent viscous damping is computed from the size of the largest loop [42]. The equivalent damping ratios are higher under the far-fault records than the near-fault records. The values of damping ratios for Short-Broad, Tall-Broad, Short-Slender, and Tall-Slender tank under the far-fault records are 29%, 25%, 22%, and 21% and under the near-fault records are 23%, 22%, 18%, and 12% respectively. The time history responses of selected tanks in

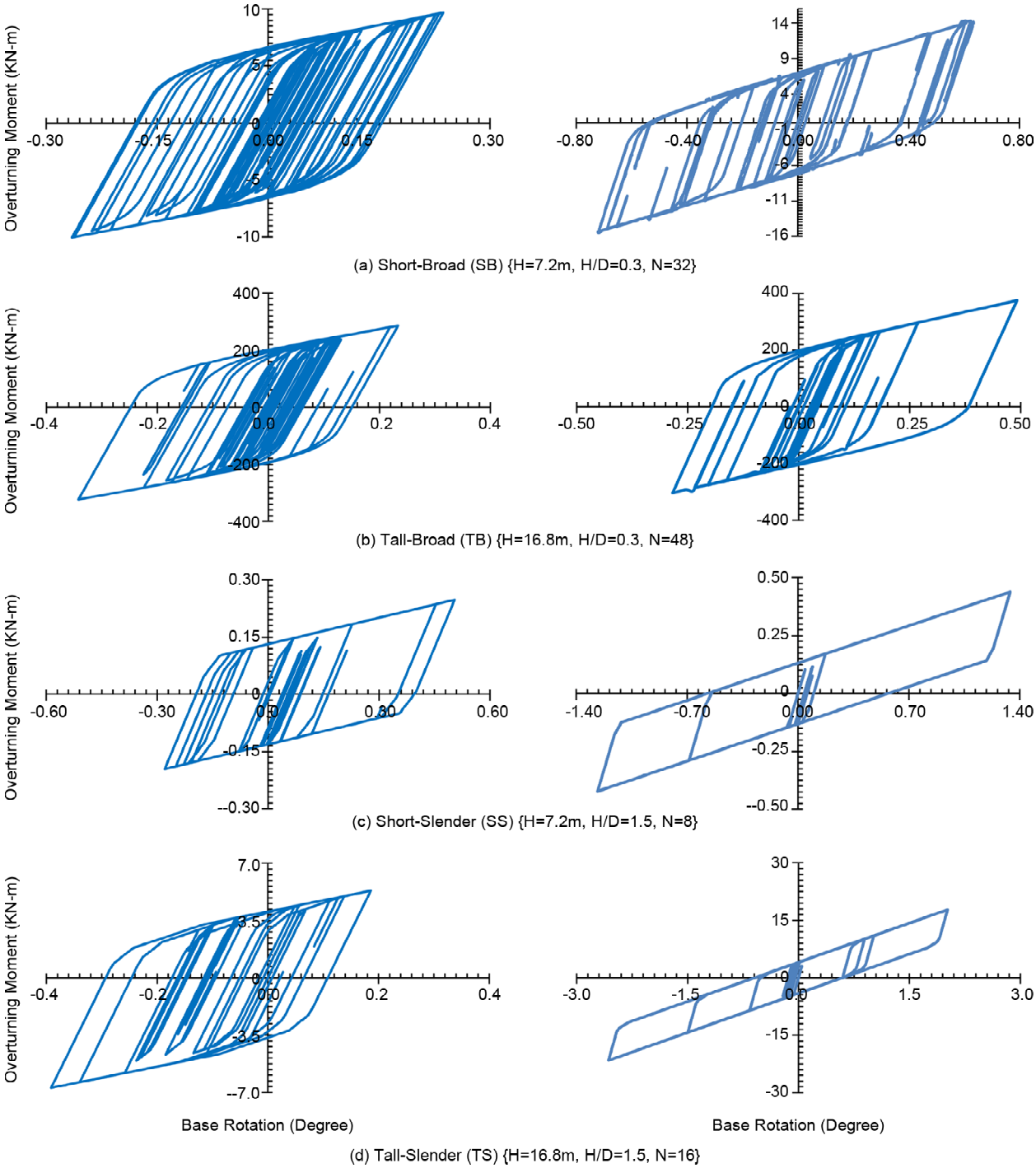

Figure 8. Moment-rotation (M-Ψ) behavior in selected isolated tanks under FF3 and NF3 input records (T_{iso} = 2.0s ,ξ_{sb} = 0.10).

Figure (7) show that the VIS performs better in the far-fault earthquake. This is due to the following facts:

1. In general, the major part of a tank seismic response is caused by the impulsive mass of the contained liquid. Because the fixed-base convective period is so long (>2sec) in selected tanks, a change from the fixed-base system to the VIS isolated system causes practically no change in either the convective period or the convective damping. Then the major portion of the overturning responses belongs to the impulsive action. When the sloshing mode of the liquid is excited, the contribution of convective mass to the seismic response of the tanks increases. Since the base isolation is mainly used to reduce the impulsive hydrodynamic pressure, the convective hydrodynamic pressure does not decrease considerably when using the isolating system, and may even increase. NF3 near-fault record is a long period earthquake and it increases the participation of convective mode in the seismic responses of the tanks, so these leads to the smaller reduction in overturning moment or lower performance of tanks under this near-fault records.
2. NF3 has higher PGV and PGV/PGA than FF3 record. The results show that these parameters have high effect on the responses and can increase the overturning moment. Also, the results indicate the high correlation between the moment res ponse reduction and higher ratio of *PGV*/*PGA*. It can be inferred from the results for all tanks that the predominant period of excitation and the fundamental period of the isolation system are the important parameters that have a significant influence on the performances of the proposed isolation system. These parameters should be reasonably selected to achieve the maximum mitigation of seismic response.

The total comparison of overturning moment responses for selected tanks is depicted in Figure (9). In each case, the responses of the VIS tank are compared with corresponding fixed-base ones. Responses of far-fault (FF) earthquakes are shown on the left side and near-fault (NF) records on the right side of the figure with their assigned ID number. It is observed that the VIS performs well under both NF and FF records and causes a significant reduction of the overturning moment, especially in slender tanks.

The normalized overturning moment is defined as the ratio of isolated to fixed base overturning moments (M_{iso}/M_{Fixed}) under the input excitation. Higher normalized overturning moment responses indicated the lower efficiency of VIS. The trends of

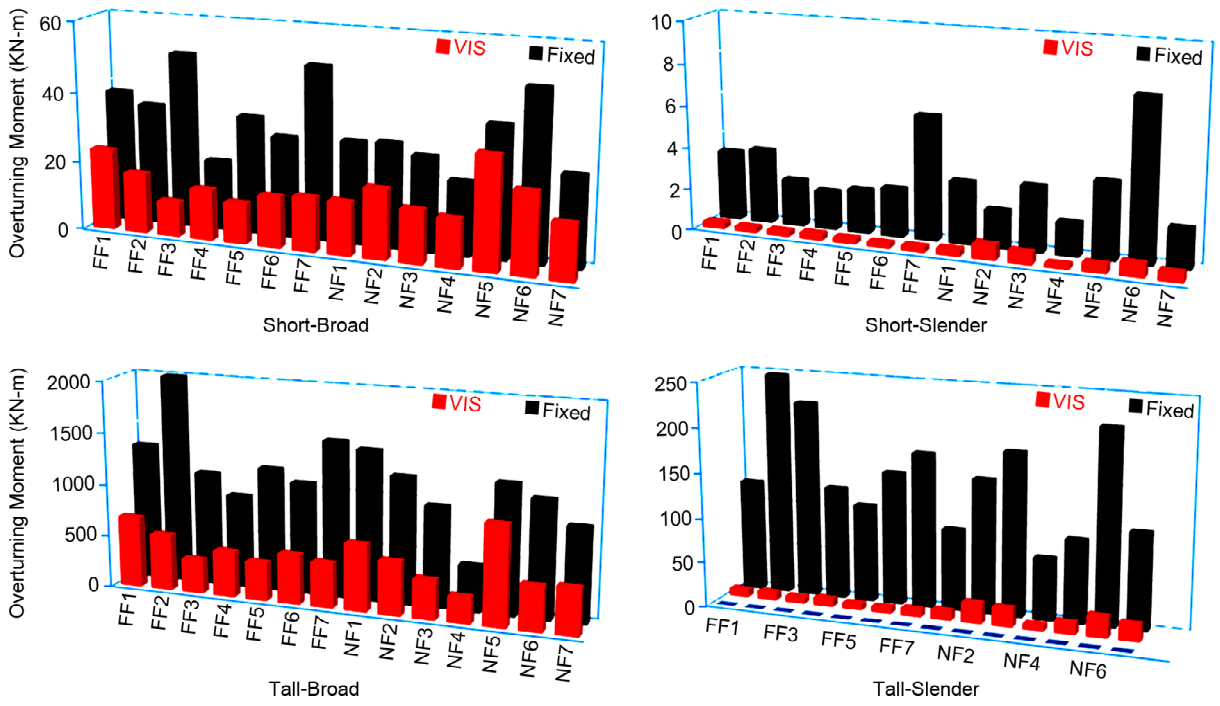

Figure 9. The comparison of overturning moment responses for selected tanks with and without VIS.

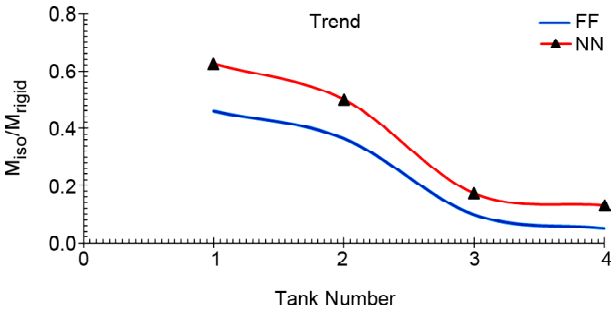

Figure 10. Trend of normalized overturning moment under the far-fault and near-fault ground motions.

the average normalized overturning moment for all near and far-fault records are depicted in Figure (10). Base isolation increases both the period and damping of the system, then the reduction in responses occurs.

It can be inferred that the slender and higher base-isolated tanks have better performances under the far-fault earthquakes rather than near records. Also due to the contribution of the high-frequency impulsive component in slender tanks, overturning moment responses are similar for NF and FF records.

8. Conclusion

The influence of near-fault and far-fault earthquake records on the seismic behavior of ASTs equipped with the proposed vertically isolation system (VIS) has been investigated in the current study. For this purpose, a set of 14 real ground motions including seven far-fault and seven pulse-like near-fault motions have been considered according to the FEMA-P695 recommendations. Because of the scaling changes, the record's peak ground velocity (PGV), which is one of the most important factors in the seismic responses of ASTs especially in near field long period records, in this study the real earthquake records without any scale factors are used as an input excitation. The VIS-equipped tanks and their associated fix-based tanks are analyzed via nonlinear time history analyses. It is assumed that the vertical isolators have bilinear force-deformation behavior. The proposed system achieves its flexibility from the uplifting and rocking motion of the shell wall and its dissipating energy from the yielding and hysteresis behavior of vertical isolators. The governing equations of motion in isolated liquid storage steel tanks are derived and solved with incremental numerical methods. To measure the effectiveness of the isolation system, the seismic overturning moment responses of isolated tanks are compared with that of the non-isolated (or fixed-based) rigid tanks. The following conclusions can be derived from the analyses:

1. The VIS performs well under both near-fault and far-fault records and causes a significant reduction in the overturning moment. Then this method can be considered as a rehabilitation method in storage tanks to mitigate the shell buckling damages during an earthquake. As depicted in Figure (10), the average reduction of overturning moment in the short-broad tank for near-fault and far-fault input excitations are about 37% and 54% respectively. In the tall-broad tank are 50% and 64%, in the short-slender tank are 83% and 90% and finally in the tall-slender tank are 87% and 93% respectively. The average of overturning moment reductions is higher for far-fault records rather than near-fault ones.
2. In general, the major part of a tank's seismic response is caused by the impulsive mass of the contained liquid. The values of damping ratios for Short-Broad, Tall-Broad, Short-Slender and Tall-Slender tank under the far-fault records are 29%, 25%, 22%, and 21% and also under the near-fault records are 23%, 22%, 18%, and 12% respectively, which is much bigger than impulsive 2% damping. Therefore, from this point of view, it can be concluded that VIS performs better in far-fault motions.
3. The near-fault earthquake excitations amplify the overall responses especially in slender tanks. In addition, because the fixed-base convective period is so long (>2sec) in selected tanks, a change from the fixed-base system to the VIS isolated system causes practically no change in either the convective period or the convective damping. Then the major portion of the overturning responses belongs to the impulsive action. Long-period near-fault earthquakes such as NF3 can excite the sloshing mode and increase the participation of convective mass in the seismic responses of the tanks. This leads to a smaller reduction in overturning moment or lower

performance of VIS under these types of near-fault records.

4. It can be inferred from the results that the higher values of PGV and PGVPGA parameters have high effects on the seismic responses and might increase the overturning moment. For example, the Imperial Valley near-fault ground motion (NF3) has higher PGV and PGVPGA than the corresponding far-fault record (FF3) and so shows less reduction in responses (see Table 1). The results show that the predominant period of excitation and the fundamental period of the isolation system are the important parameters that have a significant influence on the performance of the proposed isolation system. These parameters should be reasonably selected to achieve the maximum mitigation of seismic responses.

References

1. Cooper, T.W. (1997) *A Study of the Performance of Petroleum Storage Tanks during Earthquakes*. 1933-1995, US National Institute of Standards and Technology.

2. Fischer, E.F., Liu, J., and Varma, A.H. (2016) Investigation of cylindrical steel tank damage at wineries during earthquakes: lessons learned and mitigation opportunities. *Practice Periodical on Structural Design and Construction*, **21**(3), 04016004-1-11.

3. Erick, G., Almazan, J., Beltran, J., Herrera, R., and Sandoval, V. (2013) Performance of stainless steel winery tanks during the 02/27/2010 Maule Earthquake. *Engineering Structures*, **56**, 1402-1418.

4. Brunesi, E., Nascimbene, R. Pagani, M., and Beilic, D. (2014) Seismic performance of storage steel tanks during the May 2012 Emilia, Italy, earthquakes. *Journal of Performance of Constructed Facilities*, **29**(5), 04014137-1-9.

5. Moeini, M. and Goudarzi, M.A. (2018) Seismic damage criteria for a steel liquid storage tank shell and its interaction with demanded construction material. *Bulletin of the New Zealand Society for Earthquake Engineering*, **51**(2), 70-84.

6. Haroun, M.A. (2005) Mitigation of elephant-foot bulge formation in seismically-excited steel stor age tanks. *Proceedings of 18th International Conference on Structural Mechanics in Reactor Technology*.

7. Batikha, M., Chen, J.F., Rotter, J.M., and Teng, J.G. (2009) Strengthening metalic cylindrical sells against elephant's foot buckling with FRP. *Thin-Walled Structures*, **47**(10), 1078-1091.

8. Yazdani, M. et al. (2009) An experimental investigation into the buckling of GFRP stiffened shells under axial loading. Scientific Research and Essays 4.9.

9. Vakili, M. and Showkati, H. (2016) Experimental and numerical investigation of elephant foot buckling and retrofitting of cylindrical shells by FRP. *Journal of Composites for Construction*, **20**(4), 04015087-1-9.

10. Chen, J.F., Rotter, J.M., and Batikha, M. (2006) A simple remedy for elephant's foot buckling in cylindrical silos and tanks. *Advances in Structural Engineering*, **9**(3), 409-420.

11. Chalhoub, M.S. and Kelly, J.M. (1988) *Theoretical and Experimental Studies of Cylindrical Water Tanks in Base Isolated Structures*. Earthquake Engineering Research Center, University of California at Berkeley.

12. Shekari, M.R., Khaji, N., and Ahmadi, M.T. (2009) A coupled BE-FE study for evaluation of seismically isolated cylindrical liquid storage tanks considering fluid-structure interaction. *Journal of Fluids and Structures*, **25**, 567-585.

13. Vosoughifar, H.R. and Naderi, M.A. (2014) Numerical analysis of the base-isolated rectangular storage tanks under bi-directional seismic excitation. *British Journal of Mathematics & Computer Science*, **4**(21), 3054.

14. Li, Z.L., Li, Y., and Li, H.B. (2010) Parametric research on seismic response of large scale liquid storage tank isolated by lead-rubber bearings. *J. Sichuan Univ. (Eng. Sci. Ed.)*, **42**(5), 134-141.

15. Yang, Z.R., Shou, B.N., Sun, L., and Wang, J.J. (2011) Earthquake response analysis of

spherical tanks with seismic isolation. *Procedia Engineering*, **14**, 1879-1886.

16. Cheng, X.S., Zhao, L., and Zhang, A.J. (2015) FSI resonance response of liquid-storage structures made of rubber-isolated rectangular reinforced concrete. *Electron. J. Geotech. Eng.*, **20**(7), 1809-1824.

17. Wang, Y.P., Teng, M.C., and Chung, K.W. (2001) Seismic isolation of rigid cylindrical tanks using friction pendulum bearings. *Earthquake Eng. Struct. Dyn.*, **30**(7), 1083-1099.

18. Park, K.S., Koh, H.M., and Song, J. (2004) Cost-Effectiveness analysis of seismically isolated pool structures for the storage of nuclear spent-fuel assemblies. *Nuclear Engineering and Design*, **231**(3), 259-270.

19. Shrimali, M.K. and Jangid, R.S. (2002) Earthquake response of liquid storage tanks with sliding systems. *JSEE*, **4**(2&3).

20. Shrimali, M.K. and Jangid, R.S. (2004) Seismic analysis of base-isolated liquid storage tanks. *Journal of Sound and Vibration*, **275**, 59-75.

21. Jadhav, M.B. and Jangid, R.S. (2004) Response of base-isolated liquid storage tanks. *Shock and Vibration*, **11**, 33-45.

22. Wen, L., Wang, S.G., Du, D.S., and Xu, L.P. (2009) Controlling analysis of friction pendulum system for the seismic isolation of liquid storage tanks. *World Earthquake Eng.*, **25**(4), 161-166.

23. Zhang, R., Weng, D., and Ren, X. (2011) Seismic analysis of a LNG storage tank isolated by a multiple friction pendulum system. *Earthquake Eng. Eng. Vib.*, **10**(2), 253-262.

24. Cheng, X., Jing, W., and Gong, L. (2017) Simplified model and energy dissipation characteristics of a rectangular liquid-storage structure controlled with sliding base isolation and displacement-limiting devices. *Journal of Performance of Constructed Facilities*, **31**(5), 04017071-1-11.

25. Panchal, V.R. and Jangid, R.S. (2011) Seismic response of liquid storage steel tanks with variable frequency pendulum isolator. *KSCE J. Civ. Eng.*, **15**(6), 1041-1055.

26. Safari, S. and Tarinejad, R. (2016) Parametric study of stochastic seismic responses of base-isolated liquid storage tanks under near-fault and far-fault ground motions. *Journal of Vibration and Control*, **24**(24), 5747-5764.

27. Nikoomanesh, M.R., Moeini, M., and Goudarzi, M.A. (2019) An innovative isolation system for improving the seismic behaviour of liquid storage tanks. *International Journal of Pressure Vessels and Piping*, **173**, 1-10.

28. Moeini, M., Nikoomanesh, M.R., and Goudarzi, M.A. (2019) Vertical isolation of seismic Loads in Aboveground Liquid Storage Tanks. *Journal of Seismology and Earthquake Engineering*, **21**, 45-53.

29. Somerville, P. (2000) Characterization of near field ground motions. *Proceedings of the US-Japan Workshop: Effects of Near-Field Earthquake Shaking*, San Francisco, March 2000.

30. Bolt, B.A. (2004) Seismic input motions for nonlinear structural analysis. *ISET Journal of Earthquake Technology*, **41**, 223-232.

31. Orozco, G. and Ashford, S.A. (2002) *Effects of Large Pulses on Reinforced Concrete Bridge Columns*. Pacific Earthquake Engineering Research Center, PEER Report 2002/23, Berkeley: College of Engineering, University of California, Berkeley.

32. Somerville, P., Smith, N., Graves, R., and Abrahamson, N. (1997) Modification of empirical strong motion attenuation relations to include the amplitude and duration effects of rupture directivity. *Seismological Research Letters*, **68**, 199-222.

33. Mavroeidis, G.P., Dong, G., and Papageorgiou, A.S. (2004) Near-fault ground motions, and the response of elastic and inelastic single-degree-of-freedom (SDOF) systems. *Earthquake Engineering and Structural Dynamics*, **33**, 1023-1050.

34. The Pacific Earthquake Engineering Research Center (PEER), PEER Ground Motion Database, http://peer.berkeley.edu/.

35. Federal Emergency Management Agency (FEMA P695 / 2009) Quantification of Building Seismic Performance Factors.

36. Bazrafshan, A. and Khaji, N. (2016) Seismic response of base-isolated high-rise buildings under long-period ground motions. *Modares Civil Engineering Journal*, **16**(2), 41-52.

37. Veletsos, A.S. and Tang, Y. (1990) Soil-structure interaction effects for laterally excited liquid-storage tanks. *Earthquake Engng. Struct. Dyn.*, **19**(4), 473-496.

38. Kalantari, A., Nikoomanesh, M.R., and Goudarzi, M.A. (2019) Applicability of mass-apring models for seismically isolated liquid storage tanks. *Journal of Earthquake and Tsunami*, **13**(01), 1-17.

39. Liu, T. (2014) *Equivalent Linearization Analysis Method for Base-Isolated Buildings*. A Dissertation in University of Trento.

40. Rosenblueth, E. and Herrera, I. (1964) On a kind of hysteretic damping. *Journal of Engineering Mechanics Division*, ASCE, **90**(4), 37-48.

41. Kelly, J.M. (1986) Aseismic base isolation: review and bibliography. *Soil Dynamics and Earthquake Engineering*, **5**, 202-216.

42. Chopra, A.K. (1995) *Dynamics of Structures: Theory and Applications to Earthquake Engineering*. Prentice Hall, Inc., Englewood Cliffs, N.J.